PNAS

Supporting Information for

Metabolome-wide association study on ABCA7 indicates a role for ceramide metabolism in Alzheimer's disease

Abbas Dehghan[1-3*], Rui Climaco Pinto[1, 3], Ibrahim Karaman[1,3], Jian Huang[1, 3, 4], Brenan R Durainayagam[1, 3, 5], Mohsen Ghanbari[6], Areesha Nazeer[5], Qi Zhong[3, 5], Sonia Liggi[5], Luke Whiley[7, 8], Rima Mustafa[1], Miia Kivipelto[9-11], Alina Solomon[10-12], Tiia Ngandu[11, 13], Takahisa Kanekiyo[14], Tomonori Aikawa[14], Carola I. Radulescu[3], Samuel J. Barnes[3], Gonçalo Graça[15], Elena Chekmeneva[16, 17], Stephane Camuzeaux[16, 17], Matthew R Lewis[17, 18], Manuja R Kaluarachchi[3, 5], M Arfan Ikram[6], Elaine Holmes[3, 5, 7-8], Ioanna Tzoulaki[1-3,18], Paul M Matthews[3,19, 20], Julian L Griffin[3, 5, 21], Paul Elliott[1-3, 20, 22-23*]

Affiliations:

[1]Department of Epidemiology and Biostatistics, School of Public Health, Imperial College London; Norfolk Place, London, UK.

[2]MRC Centre for Environment and Health, School of Public Health, Imperial College London; Norfolk Place, London, UK.

[3]UK Dementia Research Institute at Imperial College London; Burlington Danes Building, Hammersmith Hospital, DuCane Road, London W12 0NN UK.

[4]Singapore Institute for Clinical Sciences (SICS), Agency for Science, Technology and Research (A*STAR); Singapore.

[5]Biomolecular Medicine, Division of Systems Medicine, Department of Metabolism, Digestion and Reproduction, Imperial College London; London, United Kingdom.

[6]Department of Epidemiology, Erasmus University Medical Center; Rotterdam, the Netherlands.[7]Australian National Phenome Centre, Computational and Systems Medicine, Health Futures Institute, Murdoch University; Harry Perkins Building, Perth, Western Australia 6150, Australia.

[8]Perron Institute for Neurological and Translational Science; Nedlands, Western Australia 6009, Australia.

[9]Institute of Public Health and Clinical Nutrition, University of Eastern Finland; Kuopio, Finland.

[10]Ageing Epidemiology (AGE) Research Unit, School of Public Health, Imperial College London; London, UK.

[11]Division of Clinical Geriatrics, Center for Alzheimer Research, Department of Neurobiology, Care Sciences and Society; Karolinska Institutet, Stockholm, Sweden.

[12]Institute of Clinical Medicine, Neurology, University of Eastern Finland; Kuopio, Finland.

[13]Department of Public Health and Welfare, Population Health Unit, Finnish Institute for Health and Welfare (THL); Helsinki, Finland.

[14]Department of Neuroscience, Mayo Clinic; 4500 San Pablo Road, Jacksonville, FL 32224, USA.

[15]Section of Bioinformatics, Division of Systems Medicine Department of Metabolism, Digestion and Reproduction, Faculty of Medicine, Imperial College London; London, UK.

[16]National Phenome Centre, Imperial College London; London W12 0NN, United Kingdom.

[17]Section of Bioanalytical Chemistry, Division of Systems Medicine, Department of Metabolism, Digestion and Reproduction, Imperial College London; London, United Kingdom.

[18]Department of Hygiene and Epidemiology, University of Ioannina Medical School, University Campus Road 455 00; Ioannina, Greece.

[19]Department of Brain Sciences, Imperial College London; London, UK.

[20]NIHR Imperial Biomedical Research Centre, Imperial College London; London, UK.

[21]The Rowett Institute, Foresterhill Campus, University of Aberdeen, Aberdeen, UK.

[22]British Heart Foundation Centre of Research Excellence, Imperial College London; London, UK.

[23]NIHR Health Protection Research Unit in Chemical and Radiation Threats and Hazards, Imperial College London; London, UK.

Corresponding author

Professor Paul Elliott, MRC Centre for Environment and Health, Department of Epidemiology and Biostatistics, School of Public Health, Imperial College of Science Technology and Medicine, London W2 1PG, United Kingdom

Email: p.elliott@imperial.ac.uk

Abbas Dehghan MD PhD, Department of Epidemiology & Biostatistics, School of Public Health,

Imperial College of Science Technology and Medicine, London W2 1PG, United Kingdom

Email: a.dehghan@imperial.ac.uk

This PDF file includes:

Supplementary methods
Supplementary results
Footnotes for Supplementary Table 2
Figures S1 to S7
SI References

Other supporting materials for this manuscript include the following:

Datasets S1 to S19

Supplementary methods

NAPE synthesis

The protocol for the synthesis of NAPEs was adapted from Basit et al.[1] For the synthesis of NAPE(P-18:0/20:4/16:0), NAPE(P-18:0/20:4/18:1), and NAPE(P-18:0/20:4/18:0), 1 mg (0.00133 mmol) of 1-(1Z-octadecenyl)-2-arachidonoyl-sn-glycero-3-phosphoethanolamine (PE(P-18:0/20:4), Avanti Polar Lipids) was aliquoted as 1 mL of 1 mg/mL supplied solution in chloroform to a precooled glass vial, and 0.55 mg of triethylamine were added in gently, stirring the mixture in the vial. An appropriate acyl chloride (16:0, 18:1 or 18:0, 0.0053 mmol each) in 0.1 mL chloroform was added dropwise to the mixture. After the addition of acyl chloride was complete, the reaction mixtures were heated to 40 °C for two hours and stirred overnight at room temperature. The reactions were quenched by adding 0.2 mL of a saturated sodium bicarbonate solution. The organic layers were collected and washed with 0.3 mL of 0.01 M hydrochloric acid and 0.3 mL of brine. The reaction mixtures were dehydrated with sodium sulfate. The solution was decanted in a clean vial and dried down under the stream of nitrogen. The product was resuspended in 0.1 mL of chloroform and purified using silica gel SPE cartridges (Phenomenex) using gradient elution with chloroform/methanol (1-20% methanol) mixture. The synthesis of NAPE(P-18:0/18:1/16:0) was carried out using the same protocol with 1-(1Z-octadecenyl)-2-oleoyl-sn-glycero-3-phosphoethanolamine (PE(P-18:0/18:1), Avanti Polar Lipids) and palmitoyl chloride as starting materials.

Supplementary results

As these were young mice, we also explored the effect of ageing in a transcriptomics dataset of brain tissue from the APP/PS1 mouse (GEO GSE 86828) to examine whether ageing may perturb sphingolipid metabolism in this model of early-onset AD. OPLS-DA readily separated 7 and 18-month-old animals according to the transcriptional profile of sphingolipid metabolism and ABCA transport genes. Ageing was associated with the increased translation of Abca9, Abca1

and CerS6. Overall, these data suggest that altered sphingolipid metabolism may be a shared mechanism associated with both LOAD and EOAD, alebit a late stage of EOAD. Sphingolipid metabolism was also altered by inflammation and hence, we asked whether activation of microglia may also induce changes in sphingolipid metabolism.

Supplementary Table 2 - MWAS on 10 *ABCA7* SNPs using untargeted National Phenome Centre LC-MS platforms (LNEG, LPOS, HPOS) and Metabolon

The table is in the attached excel file.

Footnotes:

Metabolite annotation: The pairs of numbers in brackets separated by colon are the carbon chain size followed by the number of double bonds (total number of carbons and double bonds in case it is not possible to discriminate the side chains). A "/" separates the different carbon side chains in the positions (sn-1/sn-2). An "and/or" indicates that the position of the double bonds on the same carbon side chain cannot be determined (in the case of ether or vinyl-ether bond at the sn-1 position of phospholipids (for example, O- and P-species)), while a "|" shows that the two compounds of known chain composition are coeluting.

LC-MS platform: For the untargeted UPLC-MS platforms used P means plasma; H/L means HILIC/Lipid; POS/NEG means positive or negative ionisation modes. The Metabolon platforms are presented in the Metabolon metadata, thus in addition to POS/NEG they can also be defined as early/late.

Significance threshold: Each SNP has its own multiple adjustment *P*-value threshold at a metabolome-wide significance level obtained through a permutation approach, ranging from 5.38×10^{-5} to 1.01×10^{-4}.

Ion type: Square brackets [ ] are used to show ion species detected with its charge (positive or negative) following the brackets. The notation inside the parenthesis (M+n), where n=1,2,3, is used to indicate the isotopic signals that are detected in high-resolution mass spectra along with the main ions of different types.

Annotation confidence level: This is assigned according to Sumner et al., 2007.[2] MSI level 1 corresponds to identified compound compared to the authentic chemical standard analyzed in the same experimental conditions; level 2 corresponds to a putative annotation based on the comparison of analytical data to public spectral databases; level 3 corresponds to annotated class of metabolites; level 4 is for unknown.

Metabolite abbreviation: Some annotations are ambiguous in relation to the absolute identity of the metabolite as it is not possible to distinguish between multiple possible alternatives presented using these methods. The symbols *# are used to emphasize that (*) 'O-' prefix (alkyl ether substituent) and 'P-' prefix (1Z-alkenyl ether (vinyl) substituent) and (#) the position of double bonds have not been determined. The abbreviations as used elsewhere in the document are as follows: PA*: phosphatidic acid PA(O-18:1/20:4) and/or PA(P-18:0/20:4); LacCer: lactosylceramide; SHexCer: Sulfatide hexosylceramide. The five distinct NAPE metabolites are: NAPE1*: NAPE(P-18:1/18:1/16:0) and/or NAPE(O-18:0/18:1/16:0); NAPE2*#: NAPE(P-18:1/22:5/18:0) and/or NAPE(O-18:0/22:5/18:0) and NAPE(P-18:1/22:4/18:1) and/or NAPE(O-

18:0/22:4/18:1); NAPE3*: NAPE(P-18:1/20:4/16:0) and/or NAPE(O-18:0/20:4/16:0); NAPE4*: NAPE(P-18:1/20:4/18:0) and/or NAPE(O-18:0/20:4/18:0); NAPE5*: NAPE(P-18:1/20:4/18:1) and/or NAPE(O-18:0/20:4/18:1).

NAPE annotations: Although compared to the synthesized standards obtained using commercially available plasmenyl forms of starting phosphoethanolamines (PE(P-18:0/20:4) and PE(P-18:0/18:1)), these are assigned a level of confidence of 3 corresponding to metabolite class since it is impossible to distinguish plasmenyl and either form of glycerophospholipids by MS/MS.

Supplementary Figure 1. The average levels of LacCer(d18:1/24:1) measured by serum lipid negative LC-MS in the Airwave Study per copy alleles of rs3752246

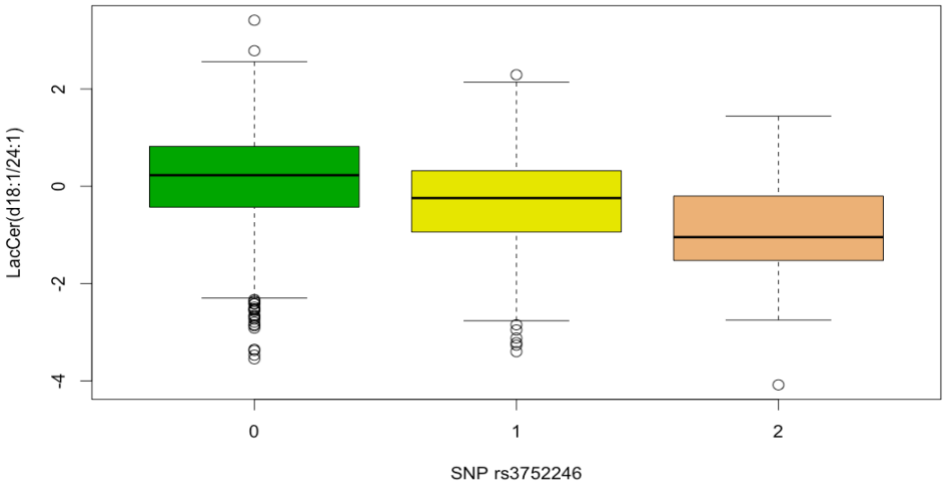

Supplementary Figure 2. Association of change in metabolite levels with change in cognitive score in FINGER trial.

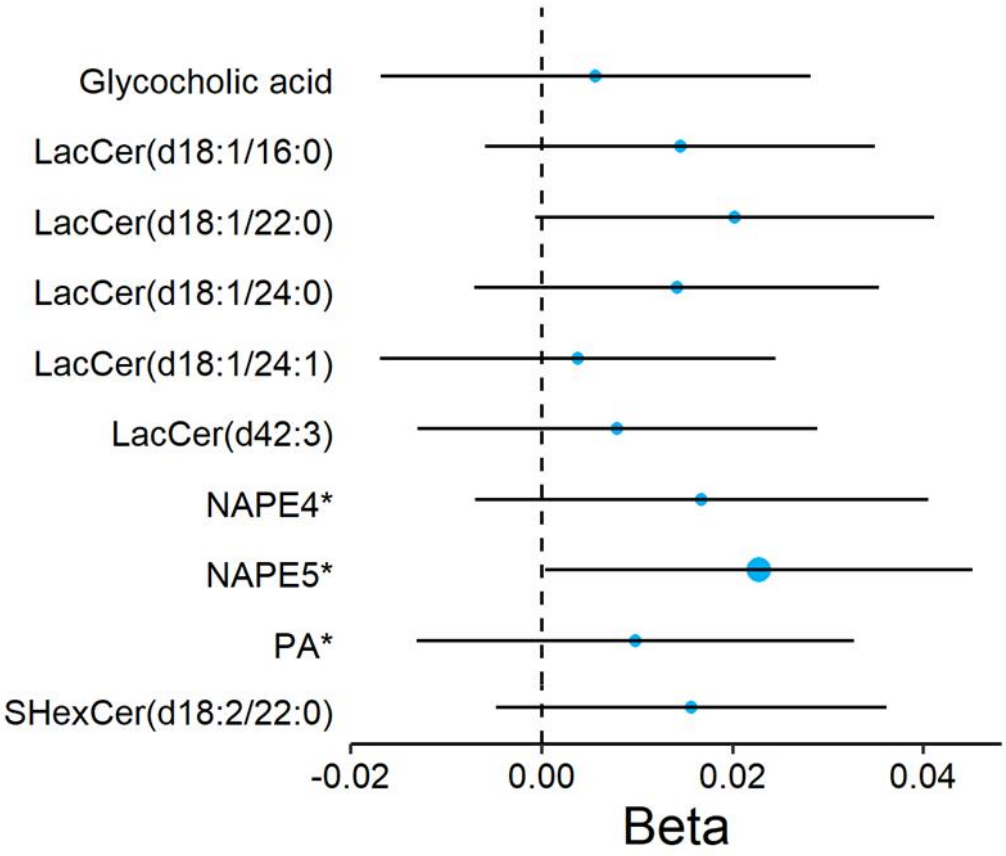

Supplementary Figure 3. **Expression quantitative trait locus (eQTL) of *ABCA7*-related SNPs in whole blood, liver, and brain tissues** (* False discovery rate<0.05; ** P<0.05/27).

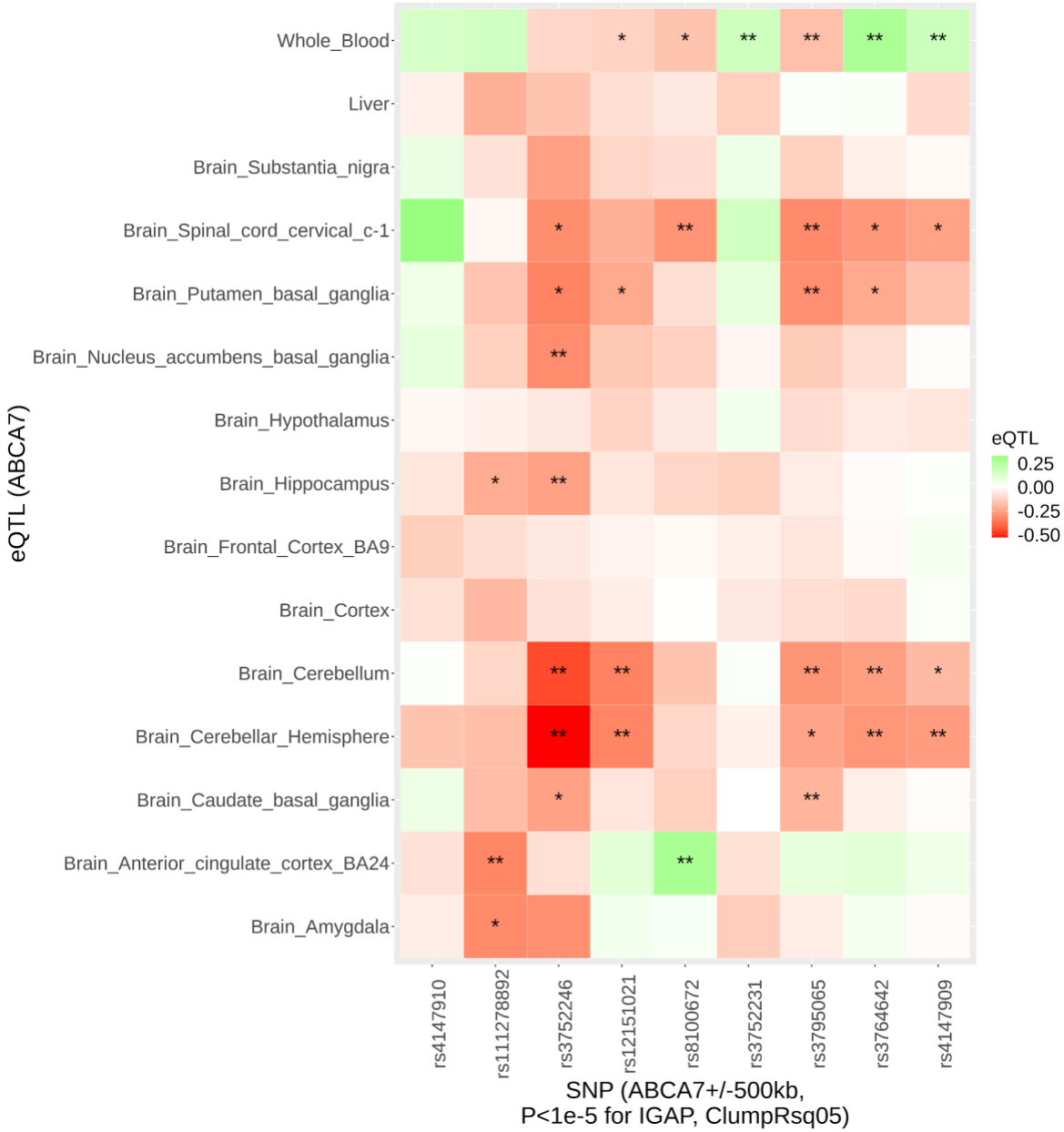

Supplementary Figure 4. a. OPLS-DA scores plot (UV scaled) of 8-week-old Abca7$^{+/-}$ and control mice brain transcriptomic data involved in sphingolipid metabolism. R^2X=91%, R^2Y=98%, Q^2=47%, passed random permutation test. **B.** Loadings plot for scores plot shown in a. Green signifies variables of the model. Blue signifies class membership in the classification matrix. **C.** OPLS-DA scores plot (UV scaled) of App/PS1 and control mice brain transcriptomic data involved in sphingolipid metabolism. R^2X=64%, R^2Y=99%, Q^2=82% **D.** Loadings plot for scores plot shown in a. Green signifies variables of the model. Blue signifies class membership in the classification matrix. (Male mice, age: 54 to 59 days).

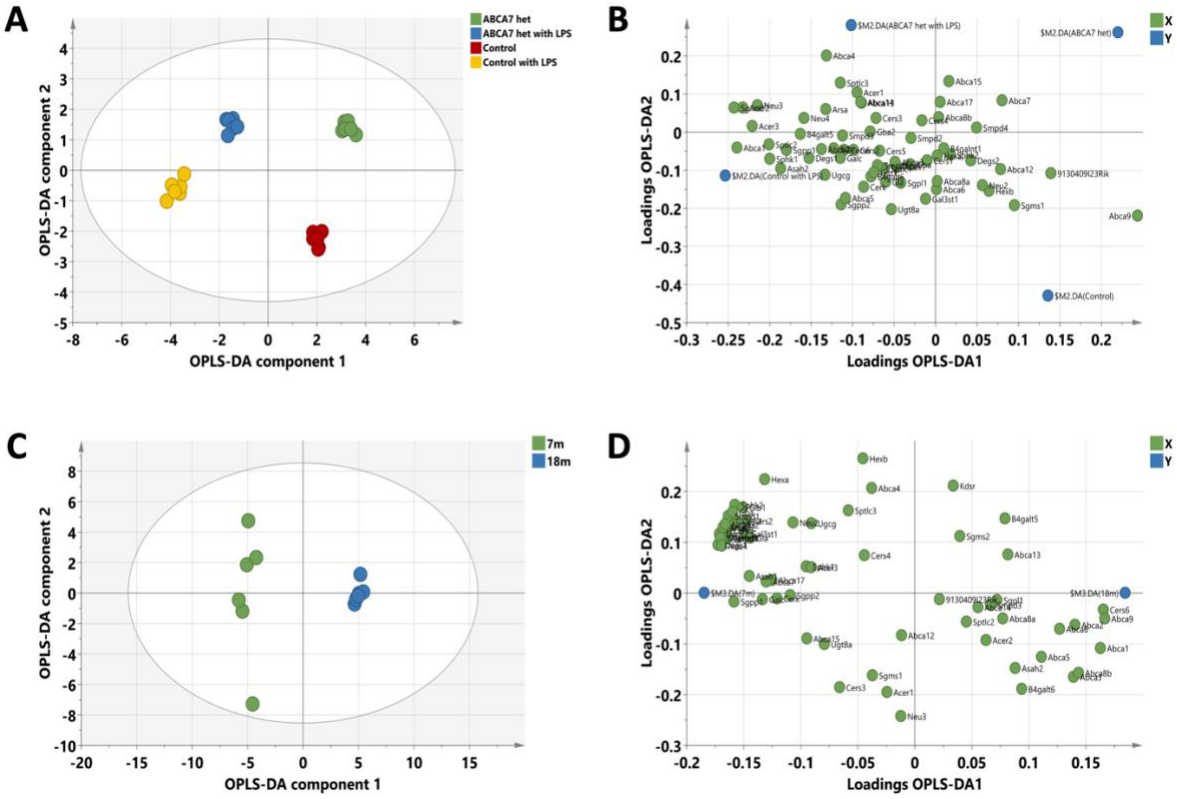

Supplementary Figure 5. OPLS-DA models to separate App^{NL-G-F} mouse brain samples from wild-type samples (10-month, female *n = 1* and male *n = 10*)**.** a) O-PLS-DA cross-validated scores plot (Pareto- scaled) of APP brain lipidomic data acquired in the positive mode. Each point represents one sample. R2X 0.936, R2Y 1, Q2 0.542, CV-ANOVA P-value 0.968. b) cross-validated permutation plot of the O-PLS-DA model built with APP brain lipidomic data acquired in the positive mode. c) O-PLS-DA cross-validated scores plot (Pareto scaled) of APP brain lipidomic data acquired in the negative mode. Each point represents one sample. R2X 0.953, R2Y 0.999, Q2 0.0165, CV-ANOVA P-value 1. d) cross-validated permutation plot of the O-PLS-DA model built with APP brain lipidomic data acquired in the negative ionization mode.

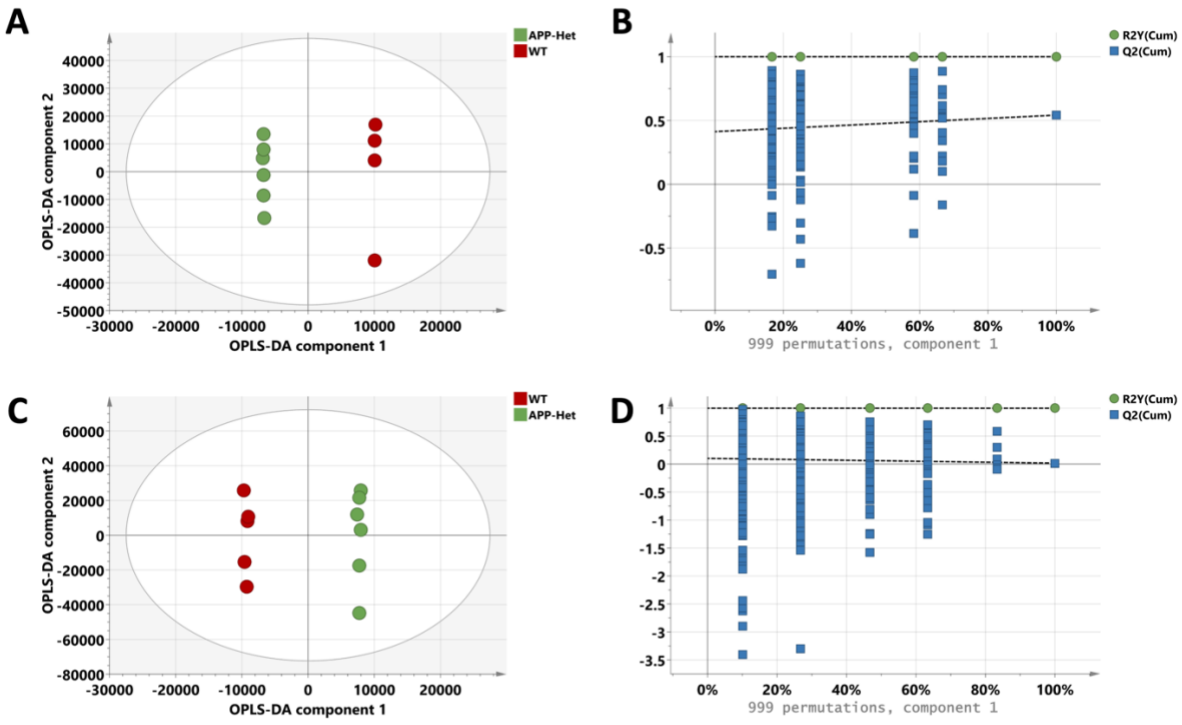

Supplementary Figure 6. High-resolution mass spectrometry fails to detect any changes in lactosyl- and hexosyl-ceramides in the mouse brain of the *App*$^{NL\text{-}G\text{-}F}$ mice (10-month, female *n = 1* and male *n = 10*)**.** Bar graphs of lactosyl- and hexosyl-ceramides detected in the brain of *App*$^{NL\text{-}G\text{-}F}$ mice. The mean + standard deviation of the mean are shown. No significant difference for all lipids according to a Student's t-test.

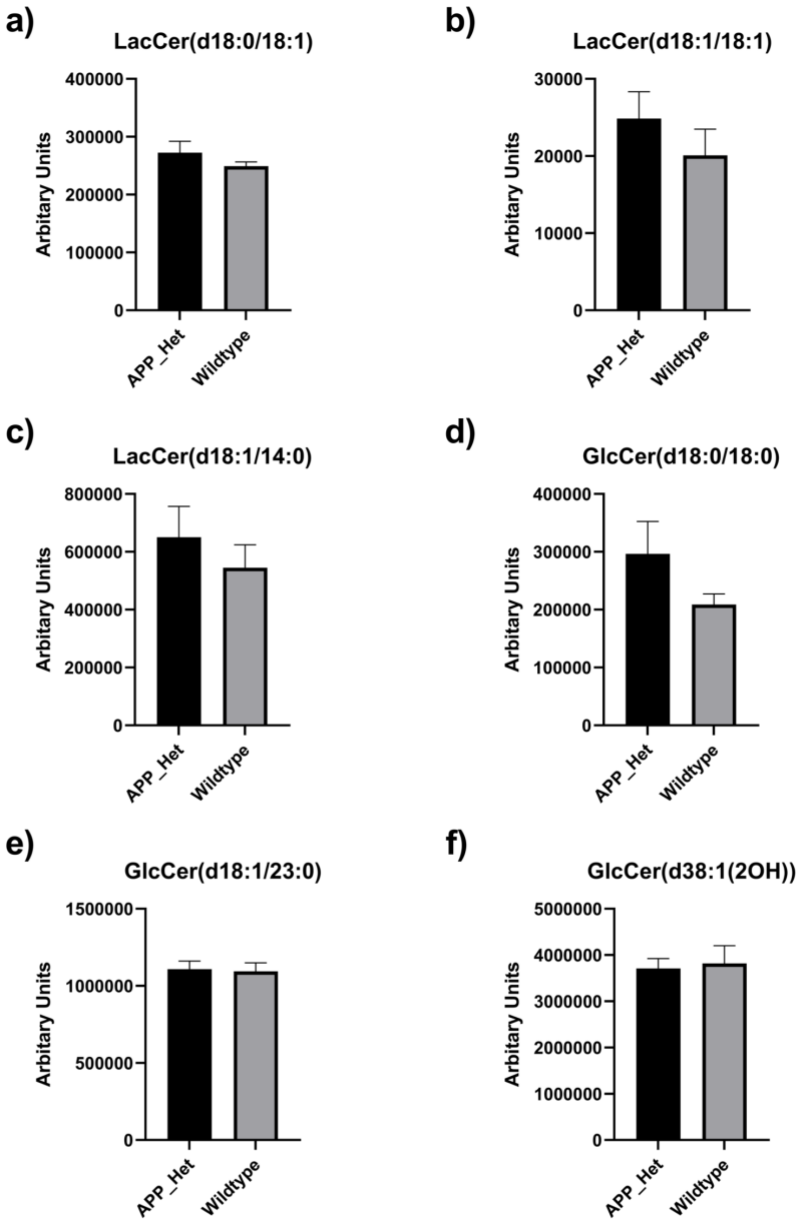

References

1. Basit, A., Pontis, S., Piomelli, D. & Armirotti, A. Ion mobility mass spectrometry enhances low-abundance species detection in untargeted lipidomics. *Metabolomics* **12**, 50 (2016).
2. Sumner, L.W.*, et al.* Proposed minimum reporting standards for chemical analysis Chemical Analysis Working Group (CAWG) Metabolomics Standards Initiative (MSI). *Metabolomics* **3**, 211-221 (2007).